Natural Resources for Human Health
eISSN: 2583-1194

Original Research

Received 14 July 2026
Revised 11 Aug 2026
Accepted 24 Aug 2026

Natural Resources for Human Health 2026, Vol. 6 (18s): 336–355

KEYWORDS:
Chitosan, Mango peel extract, Fresh chicken meat, Antioxidant activity, Antibacterial activity

Development and Characterization of Chitosan–Mango Peel Extract Films and Their Application as Active Coatings for Fresh Chicken Meat

Sourav Kumar Biswas[1], Md. Maruf Shaikh[2], Rahul Nandi[3], Alfatlawi Monyer Abdulameir Abd[4], Muhammad Hamza Sardar [5], Sehrish Murtaza[6], Tareq Nayef AlRamadneh[7], Saira Rehman[8] and Syed Izhar Ullah Shah[9]

[1]Electrical Engineering, Ingram School of Engineering, Texas State University, San Marcos, TX 78666, United States of America. E-mail: sourav@txstate.edu
[2]Electrical and Electronic Engineering, North Western University, Khulna, Bangladesh. E-mail: marufshaikh55555@gmail.com
[3]Electrical and Electronic Engineering, North Western University, Khulna. E-mail: rahulnandi4343@gmail.com
[4]Department of Veterinary Microbiology, College of Veterinary Medicine, University of Al-Qadisiyah, IRAQ. E-mail: monyerr.abd@qu.edu.iq
[5]Department of Applied Sciences, National Textile University Faisalabad. E-mail: sardarhamza677@gmail.com
[6]Institute of Molecular Biology & Biotechnology, The University of Lahore. E-mail: blues.uol.imbb@gmail.com
[7]Faculty of Allied Medical Sciences, Hourani Center for Applied Scientific Research, Al-Ahliyya Amman University, Amman, Jordan. E-mail: t.alramadneh@ammanu.edu.jo
ORCID: https://orcid.org/0000-0001-6543-5521
[8]Faculty of Pharmaceutical Sciences, Lahore University of Biological and Applied Sciences, Lahore, Pakistan. Email: Gillsaira@yahoo.com
[9]Higher Institution Centre of Excellence (HiCoE), Borneo Marine Institute, Universiti Malaysia Sabah, 88400, Kota Kinabalu, Sabah, Malaysia. Email: izharbiotech@gmail.com
Corresponding Author: Gillsaira@yahoo.com

ABSTRACT: Active chitosan-based coatings containing plant-derived bioactive compounds may enhance the storage stability of fresh poultry meat. In this study, a chitosan–mango peel extract (MPE) film was developed and its physicochemical, structural, functional and preservation properties were evaluated. The chitosan films with different concentrations of MPE were characterized in terms of their thickness, opacity, moisture content, color, water vapor permeability, swelling, solubility, antioxidant and antibacterial activities, surface morphology, thermal behavior, and mechanical properties. The coatings were then applied to fresh chicken breast meat and assessed for 12 days of refrigerated storage (4 ± 1°C). We evaluated meat quality using pH, water retention capacity, TBARS, and total viable count (TVC). The incorporation of MPE had a significant effect on the properties of the films ($p<0.001$). Increasing MPE concentration significantly increased film thickness, opacity, swelling, solubility, antioxidant activity, and antibacterial activity, whereas moisture content and water-vapor permeability decreased. The water vapor permeability of CS-MPE3 was reduced by 38.7% when compared to neat

chitosan. FTIR analysis suggested that there were changes in the hydrogen-bonding environment of the chitosan matrix, whereas XRD analysis showed changes in the structural ordering. SEM showed an increase in the surface roughness at higher MPE concentrations. The pH, water retention, TBARS and TVC parameters were significantly influenced by coating treatment, storage time and their interaction for meat storage ($p < 0.001$). Among the formulations evaluated on chicken meat, CS-MPE2 showed the lowest microbial counts and lipid oxidation and the highest water retention during refrigerated storage. The chitosan–MPE coatings in general, and especially CS-MPE2, showed promise as biodegradable active coating systems to preserve the physicochemical and microbiological quality of fresh chicken meat in refrigerated storage.

INTRODUCTION

As the demand for fresh and minimally processed food becomes increasingly greater, packaging systems must preserve the quality of the food while also minimizing environmental impact from the use of petroleum-based plastics. Fresh chicken meat has a high moisture content and nutrient level, which makes it very susceptible to deterioration during refrigeration, as microbes and other physicochemical reactions can thrive in the moisture and nutrient content. As a result, active packaging technologies that can react with food and/or its surrounding environment have become more and more attractive as alternatives and/or supplements to passive packaging systems (Yildirim et al., 2018; Shin et al., 2022). Natural polymers that can be used as biodegradable films and edible coatings are investigated as sustainable methods to ensure quality and prolong the shelf life of foods. Chitosan has great potential for application in active food packaging as a natural biopolymer due to its film-forming ability, biodegradability, biocompatibility, and antimicrobial activity. Chitin, which is a major component of crustacean shell waste, is deacetylated to generate chitosan, which has the potential to valorize food-processing by-products (Hamed et al., 2016). Its amino and hydroxyl groups can be used in intermolecular interactions; its ability to form films, in addition to its mechanical, barrier and antimicrobial properties, can be useful (Aider, 2010; Cazón and Vázquez, 2019; Roy et al., 2026). Some potential limitations of chitosan film may be due to moisture sensitivity, water-vapor barrier properties, flexibility and antioxidant functionality. The incorporation of plant extracts, phenolic compounds and essential oils and other bioactive ingredients has thus been considered to enhance the functional properties of chitosan-based films (Kerch, 2015; Salgado et al., 2015; Priyadarshi et al., 2018; Mujtaba et al., 2019; Khan et al., 2026d). Bi et al. (2019) found that incorporating proanthocyanidins increased the antioxidant and antimicrobial properties of chitosan films and altered their physical, mechanical, and thermal properties. Sarfraz et al. (2024) highlighted similar multifunctional benefits of natural additives in chitosan-based packaging. Mango (*Mangifera indica L.*) peel has been identified as a potential source of natural bioactive compounds in the above applications. Mango processing produces a significant amount of peel, which is rich in phenolic compounds, flavonoids, carotenoids and other components with antioxidant properties (Ajila et al., 2007; Marçal & Pintado, 2021; Khan et al., 2026a; Sikapuria et al., 2026). The use of MPE in biodegradable packages may, therefore, help valorize mango agro-industrial by-products and contribute to the development of functional food-packaging systems. Kanatt and Chawla (2018) proved the antioxidant and antibacterial activities of MPE-contained films and the prolonged refrigerated shelf life of minced chicken meat. Likewise, the addition of MPE to fish-gelatin films enhanced certain physical, barrier, mechanical, and antioxidant attributes. Additionally, the antioxidant, antimicrobial, optical, and barrier properties of mango by-products in biopolymer films have been shown to be promising in recent studies (Cheng et al., 2021; Zhong et al., 2026; Khan et al., 2026c). Mango peel-derived material has also been added to the chitosan film, which further shows its feasibility for active packaging applications (Adilah et al., 2018; Ponnusamy et al., 2025). These complementary functional properties can be achieved by a combination of chitosan and MPE. Chitosan can act as a film-forming matrix to give structural properties to the films and may give intrinsic antimicrobial activity, while the other phenolic compounds and bioactive compounds present in MPE may be used to impart other antioxidant and antimicrobial properties to the films. Other properties than film thickness that can be affected by MPE incorporation are opacity, moisture content, water-vapor permeability, swelling, solubility, mechanical properties, thermal stability and surface morphology. These properties are crucial as an effective active packaging must be both biologically functional and structurally stable (Cazón and Vázquez, 2019; Ponnusamy et al., 2025). The same finding was observed by Rambabu et al. (2019) when using mango leaf extract and incorporating it into chitosan films; changes in thickness, antioxidant activity, moisture and mechanical properties were observed. A favorable application system for evaluating these active coatings is fresh chicken meat because microbial proliferation and lipid oxidation are important factors contributing to the freshness of

chicken meat during refrigerated storage. Delayed microbial growth, lipid oxidation, and other deterioration processes have been previously reported during refrigerated storage of chicken meats using chitosan-based coatings (Shin et al., 2022; Khan et al., 2026b). Similarly, the chitosan biocomposite films with natural extracts have been found to inhibit microbial growth, lipid oxidation and pH rise in fresh poultry. While chitosan films loaded with different plant extracts have been studied on a large scale, the information regarding systematically characterized chitosan–MPE films on fresh chicken meat is limited. The present study was designed to prepare and characterize chitosan–MPE composite films and investigate their potential as active packaging films for fresh chicken meat during refrigerated storage. The structural, morphological, optical, barrier, antioxidant and antimicrobial properties, thermal and mechanical properties, were measured for the film, and during storage under refrigerated conditions, the coated chicken meat was evaluated for pH, water retention, lipid oxidation and total viable microbial count.

MATERIALS AND METHODS

Materials

The chitosan used (degree of deacetylation ≥95%, molecular weight 100,000–700,000 Da, viscosity 50–200 mPa·s) was purchased from Dalian Meilun Biotechnology Co., Ltd., China. The MPE was prepared in-house from the fresh peels of Chaunsa variety mangoes, which are brownish-yellow in color and in powder form. The total polyphenol concentration of the prepared extract was measured by the Folin-Ciocalteu method. 2,2-Diphenyl-1-picrylhydrazyl (DPPH) and 2,2'-azinobis(3-ethylbenzothiazoline-6-sulfonic acid ammonium salt) (ABTS) were purchased from Sigma-Aldrich (St. Louis, MO, USA). Glacial acetic acid, trichloroacetic acid (TCA), thiobarbituric acid (TBA), butylated hydroxytoluene (BHT), nutrient agar, tryptone and yeast extract were purchased from the Sinopharm Chemical Reagent Co., Ltd. (Shanghai, China). *Escherichia coli* ATCC 25922 and *Staphylococcus aureus* ATCC 29213 were obtained. In all experiments, fresh chicken breast meat was bought from the local certified supplier of meat on the day of each experiment.

Preparation of Mango Peel Extract

The peels of fresh Chaunsa mangoes were washed with distilled water, dried at 50°C for 48 h and ground to a fine powder. The mango peel powder was extracted by stirring it with 500 mL of 70% ethanol for 2 h at 60°C. The extract was filtered through Whatman No.1 filter paper and later concentrated under reduced pressure using a rotary evaporator at 45°C. The concentrated extract was then freeze-dried in order to get powdered MPE. The total polyphenol content was measured by the Folin–Ciocalteu method and reported as mg gallic acid equivalents (GAE) per g dry extract.

Preparation of Chitosan–MPE Coating Solutions and Films

Chitosan stock solution was prepared at 3% (w/w) by dissolving 1.50 g chitosan in 2% (v/v) aqueous glacial acetic acid and making up the batch to 50 g of deionized water. MPE was added to chitosan at 0, 1, 2 and 3% (w/w of chitosan), i.e., 0, 15, 30 and 45 mg MPE/1.50 g chitosan, respectively. MPE was first dispersed in a small amount of deionized water and added to the chitosan solution. The mixtures were stirred at room temperature (200 rpm, 30 min) and then treated with ultrasound (400 W, 30 min). The solutions obtained were left to stand for 2 h for degassing. The formulations were named CS, CS-MPE1, CS-MPE2 and CS-MPE3. To prepare the films, 50 g of each coating solution was poured onto a 9-cm diameter Petri dish and allowed to dry for 24 hours at 60°C. The resulting films were given 48 hours of conditioning at 25°C and 75% RH prior to characterization. Three batches of film were prepared independently on three preparation days for each formulation and each batch was treated as one experimental replicate (n = 3). If more than one technical measurement was made on the same set of films, the average of these measurements was used in the statistical analysis while the film batch itself was the experimental unit.

Characterization of Composite Films

ATR-FTIR Analysis

ATR-FTIR spectra were acquired on a Nicolet iS50 FTIR spectrometer with an ATR accessory (Thermo Fisher Scientific, USA). A total of 64 scans with a resolution of 4 cm^{-1} were collected in the 4000-400 cm^{-1} range. A representative film from each formulation was analyzed. Structural interpretation was carried out qualitatively by using FTIR spectra, which were not statistically compared.

XRD Analysis

The X-ray diffraction patterns were collected under Cu-Kα radiation from a 3 kW SmartLab diffractometer (Rigaku, Tokyo, Japan). The instrument was run with 40 kv and 40 mA. The diffraction patterns were collected over the range of 2θ from 5° to 40°, with a scan rate of 2°/min. A single representative film from each formulation was analyzed. The X-ray diffraction data were interpreted qualitatively.

Thickness, Opacity, and Moisture Content

The thickness of the films was measured at five positions on each specimen with a digital micrometer (EVERTE, China) which included a central position and four peripheral positions. The five measurements were taken and averaged to give one thickness value for each replicate of the film. Each formulation was tested with three batches of film made independently

The opacities were measured after being scanned at 600 nm with a UV–visible spectrophotometer (Lambda 365, PerkinElmer, USA) on 1 × 4 cm film strips. An empty cuvette was used as the reference. Opacity was determined by this equation:

$$O = \frac{A600}{d}$$

O is opacity ($A \cdot mm^{-1}$), A600 is absorbance at 600 nm, and d is the thickness of the film (mm).

Moisture content was determined by taking 1 × 4 cm film strips and weighing them before drying to determine their weight and then drying at 105°C for 12 h to determine their moisture content. The moisture content was defined as:

$$Moisture\ content\ (\%) = [(Mw - Md) / Mw] \times 100$$

Where M_w is the moisture content of the sample and M_d is the dry matter.

Color

Film color was measured using a HunterLab colorimeter (ColorFlex, Xinlian Creation Electronic Co. Ltd., Shanghai, China) after calibration with the manufacturer's reference plate. Lightness (L*), red–green (a*), and yellow–blue (b*) coordinates were recorded.

Chroma was calculated as:

$$C = \sqrt{[(a)^2 + (b)^2]}$$

Total color difference relative to the CS film was calculated as:

$$\Delta E* = \sqrt{[(\Delta L)^2 + (\Delta a)^2 + (\Delta b)^2]}$$

Three independently prepared film batches were analyzed for each formulation. ΔE* was calculated relative to the CS reference

Water Vapor Permeability

Water vapor permeability (WVP) was determined using the desiccant method. A circular film specimen was sealed over the mouth of a glass test tube containing 2 g of pre-dried silica gel. The effective permeation area was 7.07 cm^2. The sealed tubes were placed in a desiccator at 20 ± 1 °C with a relative humidity of approximately 100% outside the test tubes. The water vapor pressure difference (ΔP) was calculated from the saturated vapor pressure of water at 20 °C (2338 Pa), assuming an internal vapor pressure of approximately zero. The samples were weighed at 2h intervals until a linear mass-gain region was established. The steady-state water vapor transmission rate was determined from the slope of the linear portion of the mass-gain curve.

WVP was calculated using the following equation:

$$WVP = \{W \times d\}/\{t \times S \times \Delta P\}$$

where **W** is the weight gain of the film (g), **d** is the film thickness (m), **t** is the time (s), **S** is the effective permeation area (m^2), and **ΔP** is the water vapor pressure difference (Pa).

Swelling Degree

After 24 h incubation at room temperature, 1 × 4 cm film specimens were weighed again after they were submerged in 50 mL distilled water (W1). Specimens were removed, surface water was carefully tapped off with filter paper, and they were weighed at that time (WF). Swelling degree was calculated as:

$$SSwelling\ degree\ (\%) = \left(\frac{(W_f - W_0)}{W_0}\right) \times 100$$

A sample of one was analyzed from each independent preparation of film, and n = 3 for each formulation.

Solubility

The film strips were weighed after first drying them at 105°C for 12 h (WI). Each strip was then placed in 50 mL distilled water and shaken for 24 h at room temperature at 100 rpm. The recovered specimens were then dried again at 105°C for 12 h and their weight (WF) was determined. The solubility of a film was determined by:

$$Solubility\ (\%) = \left(\frac{(W_i - W_f)}{W_i}\right) \times 100$$

where WI is the initial weight of the sample; WF is the final weight of the sample.

Antioxidant Activity

The film extracts were prepared by shaking 50 mg of film in 10 mL of distilled water for 4 h at room temperature and shaking at 150 rpm. The extracts were centrifuged at 5000 × g for 10 min and the supernatants were used for antioxidant analyses. For the DPPH and ABTS experiments, sample blanks were used because of the intrinsic coloration of the extracts containing MPE. DPPH radical-scavenging activity: The film extract (9 mL) was added to DPPH solution (3 mL, 1×10^{-3} mol/L) in ethanol. This mixture was vortexed for 1 min and then incubated in the dark for 30 min before measuring absorbance at 517 nm. Sample color was corrected using a sample blank which was prepared with film extract and ethanol but without the DPPH solution. The DPPH scavenging activity was determined as:

$$\boldsymbol{DPPH\ scavenging}\ (\%) = \left(\frac{(\boldsymbol{A_{DPPH} - A_{blank}})}{\boldsymbol{A_{DPPH}}}\right) \times \mathbf{100}$$

ABTS radical-scavenging activity: The ABTS solution (7 mmol/L) was combined with the potassium persulfate solution (2.45 mmol/L) in a 1:1 ratio and left to stand in the dark at room temperature for 12–16 h. The resulting solution of ABTS radical was diluted with ethanol to an absorbance of 0.70 ± 0.02 at 734 nm. The film extract (0.2 mL) was added to 3 mL ABTS working solution and left to stand in the dark for 30 min. A sample blank (extract/ethanol) was analyzed concurrently. The scavenging activity of ABTS was determined as:

$$ABTS\ scavenging\ (\%) = \left(\frac{\left(A_{control} - \left(A_{sample} - A_{blank}\right)\right)}{A_{control}}\right) \times 100$$

Hydroxyl-radical-scavenging activity: Film extract (1 mL) was added to 0.5 mL of 9 mmol/L $FeSO_4$ and 0.5 mL of 9 mmol/L salicylic acid in ethanol. Then, 5 mL of 9 mmol/L H_2O_2 was added and the mixture was incubated at 37°C for 30 min and the absorbance was measured at 510 nm. The control system (A0) and sample reaction system (Ax) were prepared in parallel with the sample background without the H_2O_2 system (Ax0). The hydroxyl-radical-scavenging activity was determined as:

$$Hydroxyl\ radical\ scavenging\ (\%) = \left(1 - \left(\frac{(A_x - A_{x0})}{A_0}\right)\right) \times 100$$

For each formulation, three film batches were analyzed separately.

Antibacterial Activity

The antibacterial properties were tested by the agar disc diffusion test against *E. coli* ATCC 25922 and *S. aureus* ATCC 29213. Each colony was placed in nutrient broth and grown for 12 h at 37°C with shaking at 140 rpm. The cultures were adjusted to

1×10^8 CFU/mL (0.5 McFarland standard). Bacterial suspension was standardized and 1 mL was spread on nutrient agar plates uniformly along the surface of the agar. The film discs were produced in-house, and the film discs were aseptically prepared, each with a diameter of 9 mm, and were placed on the inoculated surface of the agar. The plates were then incubated at 37°C for 24 hours. The inhibition halo that appeared beyond the edge of the 9-mm film disc was measured by a digital caliper. Each formulation and bacterial strain (n = 3) had three different batches of film made. The width of the clear inhibition halo extending beyond the edge of the 9-mm film disc was measured in millimeters.

SEM Analysis

Approximately 10 × 20 mm film specimens were prepared for surface and cross-sectional examination. The films were fractured by a cross-section technique after being frozen in liquid nitrogen. The samples were coated with about 10 nm of gold via sputtering and then analyzed with a scanning electron microscope, model Gemini 360, from the company ZEISS, Germany, operated at 5 kV. Surface morphology was studied at ×500 and ×2000 magnification, while the cross-sectional morphology was studied at ×1000 and ×5000 magnification.

Thermogravimetric Analysis

The film specimens (5- 8 mg) were heated from 30 to 800°C at a rate of 10°C per minute in a NETZSCH 209F3 thermogravimetric analyzer under a nitrogen atmosphere with a flow rate of 50 mL/min. The temperature corresponding to 5% mass loss (T5%) was used as the onset degradation temperature. The temperature at which peak degradation occurred was determined from the differential thermogravimetric (DTG) curves. The amount of char remaining after the process was considered as residual char content at 800°C.

Mechanical Properties

The mechanical properties were measured with a Universal Testing Machine (QJ210, Qingji, China) in accordance with ASTM D882 Thin Plastic Sheeting. Film strips of uniform dimensions were prepared and the thickness of the specimens was measured prior to testing. The tests were conducted at 25 ± 1 °C at a 20 mm/min crosshead speed, and the tensile strength (TS) and elongation at break (EAB) values were measured. Each batch of films was prepared separately and five specimens were tested for each film batch. For statistical analysis, it was necessary to use n = 3 independent experimental replicate measurements for each independent film batch, since the five technical measurements were averaged together to create one measurement for each batch of independent films. ASTM D882 applies to thin films and sheeting that are less than 1 mm thick.

Application of Chitosan–MPE Coatings to Fresh Chicken Meat

Selection of Coating Formulations

Coating solutions were prepared following the procedure. Therefore, CS-MPE3 was excluded from the chicken-meat application experiment because its high viscosity prevented uniform coating deposition under the standardized coating conditions, rather than because of inferior functional properties. The following treatments were tested on the chicken: distilled-water control (Water), CS, CS-MPE1, and CS-MPE2. The water-dipped control was introduced to take into consideration the effects of the dipping procedure.

Chicken Sample Preparation and Coating Application

Before sample preparation work surfaces and utensils were disinfected with 75% ethanol. Independent chicken carcasses were used and the breast portion was aseptically cut into approximately 25 g portions of about 3 × 4 × 1 cm in size. The pieces were washed in sterile physiological saline and then air-dried on sterile paper. One piece of any chicken was considered an independent biological replicate. Three independent chicken pieces were used for each coating treatment and storage day, for a total of three biological replicates per treatment × storage-time combination. Pieces of chicken were immersed in the coating solution for 60 seconds, removed and drained for 10 seconds. Following this, a second immersion (60 s) was carried out after 2 min. The coated samples were left at room temperature to air-dry for 30 min and then each sample was placed in a polyethylene bag and stored at 4 ± 1°C. Independent pieces of chicken were prepared for each storage time point (days 0, 3, 6, 9, and 12) since the pH, water retention, TBARS and TVC measurements were destructive. The final design thus consisted of 4×5×3 = 60 independent experimental units.

pH

The sample of chicken was homogenized by adding 27 mL of distilled water and homogenizing at 13,000 rpm for 30s. The homogenate was filtered through a double layer of filter paper and the pH was determined using a calibrated digital pH meter.

Water Retention Capacity

A 1-g sample of chopped chicken was placed in a centrifuge tube containing 3 g of pre-weighed filter paper and centrifuged at 10,000 × g for 10 min at 4°C. The sample was immediately removed from the filter paper and weighed. Water retention was expressed as the percentage of sample mass retained after centrifugation relative to the initial sample mass. The percentage of water retained in operation was determined by:

$$Water\ retention\ (\%) = \left(\frac{W_2}{W_1}\right) \times\ 100$$

W1 is the mass of the sample before centrifuging, and W2 is the mass of the sample after centrifuging. This is not a typical water-loss method that is employed in some water retention protocols, which is the reason the term "water retention" should not be used unless this is the exact method used in the study that has been validated.

TBARS

Two grams of chicken sample was homogenized in 100μL of BHT solution (0.1g BHT in 100mL absolute ethanol) and 16mL of 5% TCA solution. The homogenate was double-filtered with filter paper. 2 mL of filtrate was added to 2 mL of 0.02 mol/L TBA solution and then incubated at 70°C for 30 minutes. Absorbance was measured at 532, 508, and 600 nm. The calculation of TBARS was done by using background-corrected absorbance and the results were expressed in mg MDA equivalents/kg sample. All experimental groups were processed in the same way and corrected using the same procedure.

Total Viable Count

Five grams of chicken sample was placed in sterile physiological saline (45 mL) and homogenized aseptically, causing its concentration to be a 10^{-1} dilution. 10-fold serial dilutions were carried out in sterile saline. Plate count agar was used for appropriate dilutions and plate counts were done in duplicate. Plates were incubated for aerobic plate counts according to GB 4789.2 at 36 ± 1°C for 48 ± 2 h to allow for aerobic counts. Some plates with an appropriate number of colonies were chosen for enumeration and presented as log CFU/g. General aerobic plate counts are specified at 36 ± 1°C for 48 ± 2 h; 30 ± 1°C/72 ± 3 h is associated with aquatic products as specified in GB 4789.2-2016.

Statistical Analysis

One-way ANOVA was used to analyze film characterization variables, with film formulation as the fixed factor (CS, CS-MPE1, CS-MPE2, and CS-MPE3). Three independently prepared film batches were considered experimental replicates. Significant differences were determined using Tukey's HSD test at $p < 0.05$. For chicken-meat parameters, two-way ANOVA was performed to assess the effects of coating treatment (Water, CS, CS-MPE1, and CS-MPE2), storage time (0, 3, 6, 9, and 12 days), and their interaction. When a significant interaction was detected, simple-effects analyses followed by Tukey's HSD test were performed. Statistical analyses were conducted using SPSS version 26.0 (IBM Corp., Armonk, NY, USA), and data are presented as mean ± SD.

RESULTS AND DISCUSSION

Characterization of Chitosan–MPE Films

ATR-FTIR Analysis

The characteristic absorption bands observed in the CS film were near 3280 cm^{-1}, 1540 cm^{-1}, 1070 cm^{-1}, and 1020 cm^{-1}, which are mainly due to O–H/N–H stretching vibrations, N–H bending vibrations, C–O–C and C–O stretching vibrations, respectively, attributed to the chitosan matrix. The characteristic functional groups detected for these chitosan-based films are similar to those found in other chitosan-based films and are commonly related to the polysaccharide backbone and its hydroxyl and amino groups (Elsabee and Abdou, 2013; Mujtaba et al., 2019). The chitosan-associated bands were still visible and measurable after MPE incorporation, thus chitosan being still the major structural component of the films. The O–H/N–H band was observed to shift its position from ca. 3280 cm^{-1} for CS to ca. 3320, 3375, and 3395 cm^{-1} for CS-MPE1, CS-MPE2

and CS-MPE3, respectively (Figure 1). Such shifts may reflect changes in the local chemical environment and hydrogen-bonding interactions following incorporation of MPE into the chitosan matrix. Similar modifications in FTIR spectra after the addition of plant extracts into chitosan films are reported in the literature, likely due to intermolecular interactions, such as hydrogen bonding, that alter the chemical environment of the polymer chains (Wang et al., 2019). FTIR results can, however, not be used to determine a particular molecular interaction or chemical bond formation. Similar changes in the intensities of the bands at 1540 and 1070 cm-1 were also noted as the concentration of MPE increased. Spectral changes suggest modification of the molecular environment of the chitosan matrix after MPE has been incorporated, but further spectroscopic or chemical characterization would be required to determine the molecular mechanism of this modification. This conservative explanation is in line with the results from other works, which have reported that extracts from plants can induce changes in the FTIR profile of the chitosan-based composite films without forming new covalent bonds (Wang et al., 2019).

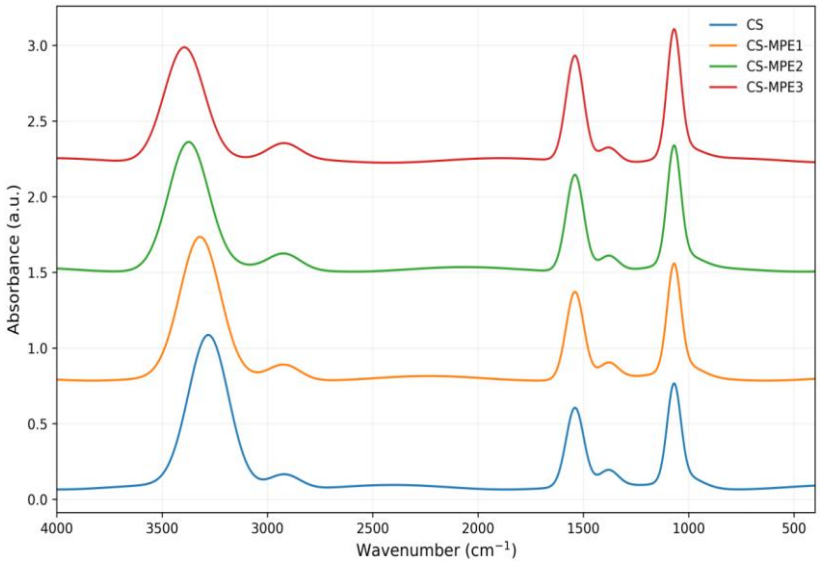


Figure 1. ATR-FTIR spectra of chitosan–mango peel extract (CS–MPE) films at different MPE concentrations.

XRD Analysis

The characteristic diffraction peaks of the CS film were observed near 2θ = 8, 11, 17, 22, which are characteristic of semi-crystalline CS (Figure 2). The semi-crystalline structure of chitosan films and the sensitivity of the diffraction pattern of the film to blending with bioactive compounds have been reported earlier (Elsabee and Abdou, 2013; Mujtaba et al., 2019). The chitosan-related diffraction peaks were still present in the films containing MPE, consistent with retention of the basic chitosan matrix structure of the chitosan matrix. The diffraction intensity suggests a reduction in structural ordering of the composite matrix with increasing MPE concentration. Other alterations in crystallinity have been reported for matrices containing plant-derived compounds, due to variations in intermolecular organization and in polymer chain packing (Wang et al., 2019). A secondary diffraction feature was found near 2θ ≈ 15° in both CS-MPE1 and CS-MPE2 and was seen to diminish in CS-MPE3. This change could be due to changed intermolecular packing after incorporation of MPE. Hence, the observations made are qualitative rather than statistical due to XRD being carried out on a single film for each formulation.

Natural Resources for Human Health
eISSN: 2583-1194

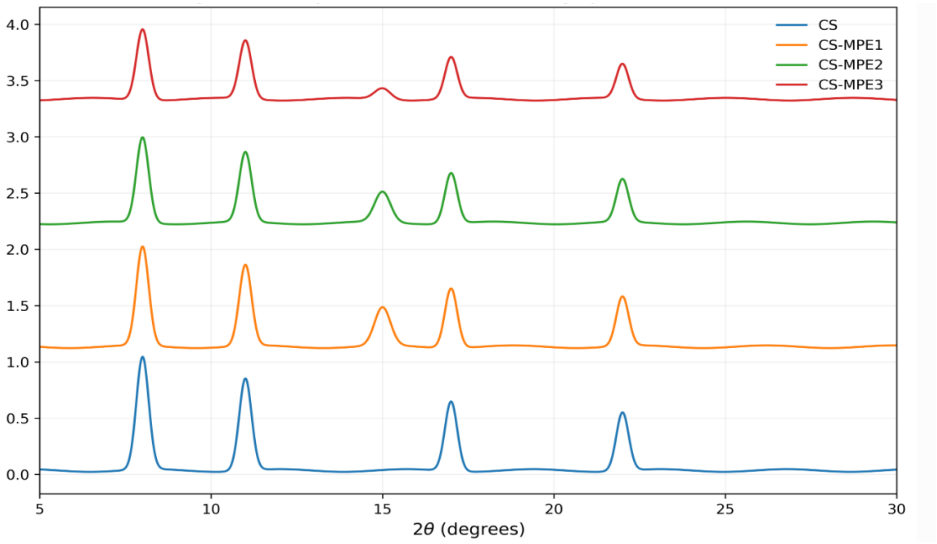


Figure 2. X-ray diffraction (XRD) patterns of chitosan–mango peel extract (CS–MPE) films at different MPE concentrations

Thickness, Opacity, and Moisture Content

The thickness, opacity, and moisture content are given in Table 1. One-way ANOVA indicated significant effects of film formulation on thickness ($F_{3,8} = 18.43$, $p < 0.001$), opacity ($F_{3,8} = 124.37$, $p < 0.001$), and moisture content ($F_{3,8} = 87.62$, $p < 0.001$). Film thickness increased progressively from 0.281 ± 0.021 mm in CS to 0.344 ± 0.025 mm in CS-MPE3. This was around 7.8, 14.6%, and 22.4% greater than CS when compared to CS-MPE1, CS-MPE2 and CS-MPE3, respectively. The rise is in accordance with the extra dry solids added from MPE incorporation. Higher thickness in the film after adding plant extracts to the chitosan film has been observed in previous studies as well (Rambabu et al., 2019; Wang et al., 2019). Opacity also increased steadily with increasing MPE concentration. The opacity increased from 0.724 ± 0.051 $A \cdot mm^{-1}$ in CS to 5.318 ± 0.541 $A \cdot mm^{-1}$ in CS-MPE3. The rise is in agreement with the addition of the coloured constituents of mango peel into the film matrix. Darker color and higher transparency of chitosan films with plant extracts have been reported (Wang et al., 2019; Rambabu et al., 2019). Mango peel also has phenolic and other pigmented phytochemical constituents that could cause changes in the optical properties of the packaging matrices (Jahurul et al., 2015; Quintana et al., 2021). Moisture content decreased from 37.84 ± 0.42% in CS to 26.15 ± 0.47% in CS-MPE3. The CS-MPE1, CS-MPE2 and CS-MPE3 had relative reductions of 19.3%, 24.8% and 30.9%, respectively. This decrease could be due to the modification of hydrophilic sites and water association within the composite matrix after MPE incorporation. The moisture content after chitosan film preparation using botanical extracts has been reported and might be influenced by the composition of botanical extracts and interactions with the chitosan matrix (Wang et al., 2019).

Table 1. Thickness, opacity, and moisture content of chitosan–MPE films (n = 3 independent film batches).

Film	Thickness (mm)	Opacity ($A \cdot mm^{-1}$)	Moisture Content (%)
CS	0.281 ± 0.021^{a}	0.724 ± 0.051^{a}	37.84 ± 0.42^{d}
CS-MPE1	0.303 ± 0.018^{ab}	3.412 ± 0.614^{b}	30.53 ± 0.58^{c}
CS-MPE2	0.322 ± 0.014^{ab}	4.763 ± 0.382^{c}	28.47 ± 0.61^{b}
CS-MPE3	0.344 ± 0.025^{b}	5.318 ± 0.541^{c}	26.15 ± 0.47^{a}

Different lowercase superscript letters within a column indicate significant differences according to Tukey's HSD test ($p < 0.05$).

Color

Color

The color parameters are shown in Table 2. Significant effects of formulation were observed for L* ($F_{3,8} = 312.47$, $p < 0.001$), a* ($F_{3,8} = 64.83$, $p < 0.001$), b* ($F_{3,8} = 187.26$, $p < 0.001$), and C* ($F_{3,8} = 143.58$, $p < 0.001$). The L* value decreased gradually as MPE was added, resulting in a darker film appearance. The a* coordinate increased, while the b* coordinate decreased significantly from CS (50.23 ± 0.71) to CS-MPE3 (7.62 ± 0.28). Therefore, incorporation of MPE changed the films from the relatively light yellowish appearance of CS to a darker brownish color. Wang et al. (2019) and Rambabu et al. (2019) reported similar changes in lightness, redness, and yellowness after incorporation of plant extracts into chitosan-based films. Chroma also decreased as MPE concentration increased, indicating lower color saturation. The observed color changes indicate that incorporation of MPE noticeably modified the visual appearance of the films. These optical changes are plausibly associated with phenolic compounds and other phytochemicals present in mango peel (Jahurul et al., 2015; Quintana et al., 2021).

Table 2. Color parameters of chitosan–MPE films (n = 3 independent film batches).

Film	L*	a*	b*	C*
CS	73.45 ± 0.62^{d}	3.51 ± 0.14^{a}	50.23 ± 0.71^{d}	50.35 ± 0.71^{d}
CS-MPE1	38.27 ± 0.48^{c}	7.84 ± 0.21^{b}	28.64 ± 0.55^{c}	29.69 ± 0.53^{c}
CS-MPE2	22.37 ± 0.35^{b}	13.52 ± 0.27^{c}	11.73 ± 0.39^{b}	17.90 ± 0.33^{a}
CS-MPE3	16.84 ± 0.29^{a}	16.43 ± 0.31^{d}	7.62 ± 0.28^{a}	18.11 ± 0.31^{a}

Different lowercase superscript letters indicate significant differences within a column ($p < 0.05$).

Water Vapor Permeability

The effect of MPE concentration on WVP was significant ($F_{3,8} = 96.74$, $p < 0.001$; Table 3). WVP decreased from 8.74 ± 0.28 × 10^{-10} g·m^{-1}·s^{-1}·Pa^{-1} in CS to 5.36 ± 0.15 × 10^{-10} g·m^{-1}·s^{-1}·Pa^{-1} in CS-MPE3. The WVP of CS-MPE1, CS-MPE2, and CS-MPE3 decreased by about 15.0%, 27.5%, and 38.7%, respectively, relative to CS. As the MPE concentration increased, water-vapor permeability decreased, indicating improved resistance of the composite films to water-vapor transfer. This effect may be associated with changes in the polymer matrix and reduced availability or mobility of hydrophilic pathways following MPE incorporation (Wang et al., 2019; Ribeiro et al., 2021). The observed behavior may be linked to the changes in matrix organization and the development of a more tortuous diffusion pathway, but this depends on the interactions between the extract constituents and polymer chains.

Swelling Degree

The swelling degree was significantly increased with MPE concentration ($F_{3,8} = 42.18$, $p < 0.001$) (Table 3). CS showed a swelling degree of 541.63 ± 58.24%, whereas CS-MPE3 exhibited 889.85 ± 44.67%. The MPE-containing films showed increased water absorption in the 24 h immersion test. This was found at the same time as the reduction in WVP, indicating that the two properties were influenced differently by the incorporation of MPEs. The differences in vapor transport and liquid-water uptake have been reported for chitosan-based active films; these properties depend on aspects of matrix structure and polymer–extract interactions (Wang et al., 2019; Muñoz-Tebar et al., 2023).

Solubility

The effect of the concentration of MPE on the solubility of films was significant ($F_{3,8} = 78.53$, $p < 0.001$; Table 3). Solubility increased from 19.84 ± 0.76% in CS to 38.77 ± 1.14% in CS-MPE3. The increases of about 68.5, 81.2, and 95.4% are calculated with respect to CS for CS-MPE1, CS-MPE2, and CS-MPE3, respectively. The rise could be due to the contribution of the water-soluble parts of MPE as well as organizational changes of the chitosan matrix. Previous studies have demonstrated that

the incorporation of plant extracts can alter the water solubility and swelling properties of chitosan films, depending on the chemistry of the extract and its concentration (Wang et al., 2019; Muñoz-Tebar et al., 2023).

Table 3. WVP, swelling degree, and solubility of chitosan–MPE films (n = 3 independent film batches).

Film	WVP ($\times 10^{-10}$ g·m^{-1}·s^{-1}·Pa^{-1})	Swelling Degree (%)	Solubility (%)
CS	8.74 ± 0.28^{d}	541.63 ± 58.24^{a}	19.84 ± 0.76^{a}
CS-MPE1	7.43 ± 0.22^{c}	726.48 ± 63.51^{ab}	33.42 ± 1.08^{b}
CS-MPE2	6.34 ± 0.19^{b}	812.37 ± 47.82^{bc}	35.97 ± 0.93^{bc}
CS-MPE3	5.36 ± 0.15^{a}	889.85 ± 44.67^{c}	38.77 ± 1.14^{c}

Different lowercase superscript letters indicate significant differences within a column according to Tukey's HSD test ($p < 0.05$).

Antioxidant Activity

The antioxidant activity of sample-blank-corrected samples is given in Table 4. Significant effects of film formulation were observed for DPPH ($F_{3,8} = 218.43$, $p < 0.001$), ABTS ($F_{3,8} = 176.82$, $p < 0.001$), and hydroxyl-radical scavenging activity ($F_{3,8} = 154.67$, $p < 0.001$). The radical-scavenging activity of the CS film was relatively low with values of 4.12 ± 0.38%, 6.23 ± 0.51%, and 8.47 ± 0.64% for DPPH, ABTS and hydroxyl-radical assays respectively. In all three antioxidant measurements, an increase in antioxidant levels was observed as a function of increased concentration of MPE. The antioxidant activities measured were the highest in CS-MPE3, at 58.74 ± 1.43, 72.36 ± 1.87 and 65.82 ± 1.54% for DPPH, ABTS and hydroxyl-radical scavenging, respectively (Figure 3). The results showed that the radical-scavenging activity of the chitosan films was significantly enhanced by the incorporation of MPE. This is consistent with the reported high phenolic compound and other antioxidant content of mango peel and with the previous studies indicating improved antioxidant activity after chitosan film incorporation of plant extracts (Jahurul et al., 2015; Moalla et al., 2021; Quintana et al., 2021; Muñoz-Tebar et al., 2023).

Table 4. Antioxidant activity of chitosan–MPE films after sample-blank correction (n = 3 independent film batches).

Film	DPPH Scavenging (%)	ABTS Scavenging (%)	Hydroxyl Scavenging (%)
CS	4.12 ± 0.38^{a}	6.23 ± 0.51^{a}	8.47 ± 0.64^{a}
CS-MPE1	28.63 ± 1.12^{b}	38.74 ± 1.43^{b}	32.56 ± 1.27^{b}
CS-MPE2	46.38 ± 1.34^{c}	58.92 ± 1.65^{c}	51.83 ± 1.38^{c}
CS-MPE3	58.74 ± 1.43^{d}	72.36 ± 1.87^{d}	65.82 ± 1.54^{d}

Different lowercase superscript letters indicate significant differences within a column ($p < 0.05$).

Natural Resources for Human Health
eISSN: 2583-1194

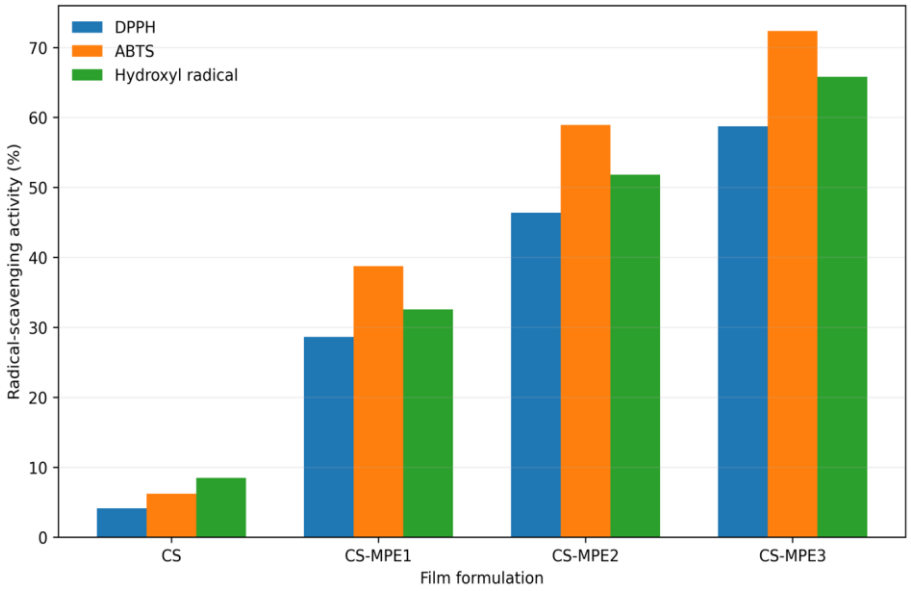


Figure 3. Antioxidant activity of chitosan–mango peel extract (CS–MPE) films determined by DPPH, ABTS, and hydroxyl radical-scavenging assays.

Antibacterial Activity

The antibacterial activity against *E. coli* and *S. aureus* is shown in Table 5. Significant effects of formulation were observed for both *E. coli* ($F_{3,8} = 143.27$, $p < 0.001$) and *S. aureus* ($F_{3,8} = 168.54$, $p < 0.001$). The CS film produced inhibition halos of 8.43 ± 0.54 and 10.27 ± 0.63 mm against *E. coli* and *S. aureus*, respectively. The inhibition halo increased progressively with increasing MPE concentration, with the largest inhibition-zone widths observed for CS-MPE3. The inhibition halo gradually grew with increasing doses of MPE, and the largest measured halos were obtained with CS-MPE3. For *E. coli*, inhibition increased from 8.43 ± 0.54 mm for CS to 18.64 ± 0.72 mm for CS-MPE3. For *S. aureus*, the corresponding increase was from 10.27 ± 0.63 mm to 21.37 ± 0.84 mm (Figure 4). The higher inhibition of *S. aureus* than that of *E. coli* is consistent with the difference in envelope structures of Gram-positive and Gram-negative bacteria. This antimicrobial activity enhancement after adding botanical extracts to chitosan films has already been described (Yuan et al., 2016; Wang et al., 2019; Muñoz-Tebar et al., 2023). Mango peel also has antibacterial activity, which is attributed to various compounds (Umamahesh et al., 2020; El-Sayed et al., 2025). The exact mechanism responsible for the increased activity, however, has not been directly studied.

Table 5. Antibacterial activity of chitosan–MPE films expressed as inhibition halo measurements beyond the 9-mm film disc (n = 3 independent film batches).

Film	E. coli (mm)	S. aureus (mm)
CS	8.43 ± 0.54^{a}	10.27 ± 0.63^{a}
CS-MPE1	13.26 ± 0.61^{b}	15.84 ± 0.74^{b}
CS-MPE2	16.43 ± 0.68^{c}	18.62 ± 0.71^{c}
CS-MPE3	18.64 ± 0.72^{d}	21.37 ± 0.84^{d}

Different lowercase superscript letters indicate significant differences within a column ($p < 0.05$).

Natural Resources for Human Health
eISSN: 2583-1194

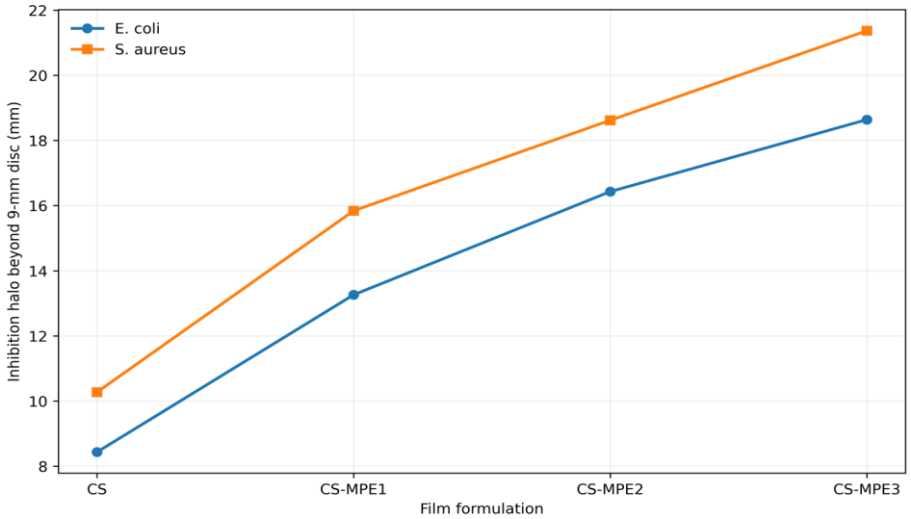


Figure 4. Antibacterial activity of CS–MPE films against *E. coli* and *S. aureus*, expressed as inhibition-zone width beyond the 9-mm disc.

SEM Analysis

The surface and cross-sectional structure of the CS film were relatively smooth and compact. For the two CS products, CS-MPE1 and CS-MPE2, the surfaces remained relatively smooth, but with some surface roughness variations (Figure 5). CS-MPE3 showed more surface irregularity and features of small particulates. The observations indicate that as MPE concentration increased, the film matrix morphology changed and could have stimulated localised concentration of the MPE components at the highest concentration. Similar morphological alterations have been reported when using other botanical extracts or bioactive compounds in chitosan films (Rambabu et al., 2019). The CS-MPE1 and CS-MPE2 were relatively sound without any apparent macroscopic voids, as seen in cross-sectional images. The morphological changes as observed by SEM support the changes in the physical and barrier properties, but do not give absolute proof of the molecular mechanism involved in the film-forming process.

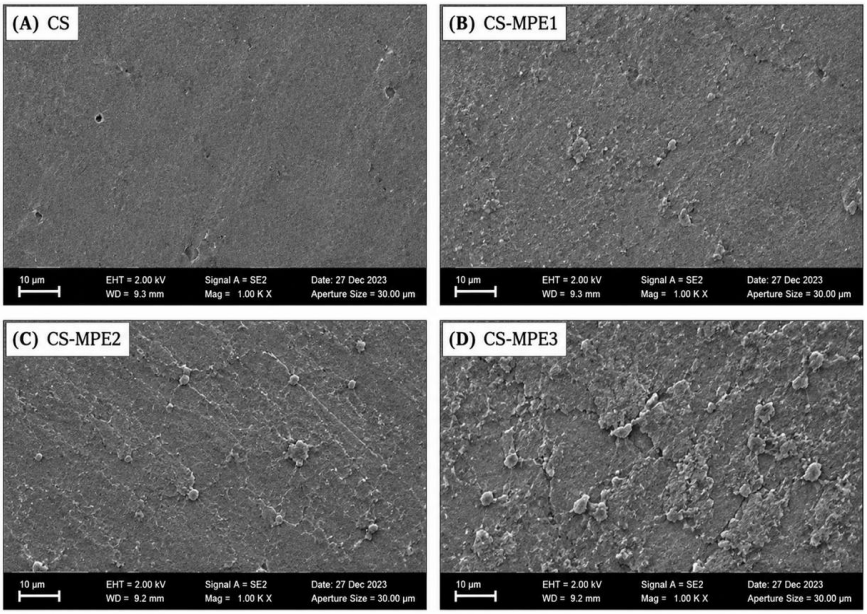


Figure 5. Scanning electron microscopy (SEM) images of chitosan–mango peel extract (CS–MPE) films showing changes in surface morphology with increasing MPE concentration.

Thermogravimetric Analysis

The films were shown to exhibit a first mass-loss phase which was correlated with water loss followed by a large thermal degradation of polymeric and organic material. The T5% value increased with CS-MPE3 from 238°C to 255°C. (Table 6) Also, the maximum degradation temperature of the major degradation stage gradually increased from 294°C to 314°C. The changes in the thermograms suggest that the thermal degradation curve of the films has been changed after MPE incorporation. The thermal properties of chitosan matrices can be modified by plant extracts, which leads to changes in the intermolecular interactions between the matrix and the plant extracts and in the organization of the matrix. The residual char content was found to be higher in CS-MPE3 compared to CS (18.3 to 27.8%). The higher residual mass could be correlated with the higher contribution of the aromatic and polyphenolic components to the thermally stable carbonaceous residues. The processes have been referred to as thermal degradation/pyrolysis, since the experiments were carried out in a nitrogen atmosphere, rather than oxidative degradation.

Table 6. Thermal degradation parameters of chitosan–MPE films.

Film	T_5%† (°C)	Tpeak, Stage II† (°C)	Residual Char at 800 °C† (%)
CS	238	294	18.3
CS-MPE1	244	301	21.7
CS-MPE2	251	308	24.6
CS-MPE3	255	314	27.8

T_5% represents the temperature corresponding to 5% mass loss. Tpeak represents the peak temperature obtained from the DTG curve.

Mechanical Properties

The mechanical properties are presented in Table 7. Film formulation significantly affected tensile strength ($F_{3,8} = 34.72$, $p < 0.001$) and elongation at break ($F_{3,8} = 28.46$, $p < 0.001$). Tensile strength increased from 18.43 ± 0.84 MPa for CS to 26.87 ± 1.12 MPa for CS-MPE2. The tensile strength for CS-MPE3 was 24.13 ± 0.97 MPa which was lower than the tensile strength of CS-MPE2. The enhancement to CS-MPE2 could be attributed to reinforcement of the matrix and intermolecular interactions after the incorporation of MPE, while the decrease in CS-MPE3 could be attributed to the increased morphological irregularity seen in SEM. Concentration-dependent variations in mechanical properties were also reported for the chitosan films loaded with botanical extracts; a moderate concentration of botanical extracts is able to reinforce the chitosan matrix whereas overloading is able to disrupt the polymer chain organization (Rambabu et al., 2019). Elongation at break decreased with progressive increase in the concentration of MPE from 42.36 ± 2.14% in CS to 28.74 ± 1.83% in CS-MPE3, suggesting a decrease in extensibility as the concentration of MPE increased. These decreases in extensibility have been reported for a few films based on chitosan when they were loaded with natural active ingredients.

Table 7. Mechanical properties of chitosan–MPE films (n = 3 independent film batches; five technical specimens averaged within each batch).

Film	Tensile Strength (MPa)	Elongation at Break (%)
CS	18.43 ± 0.84^{a}	42.36 ± 2.14^{c}
CS-MPE1	22.67 ± 0.93^{b}	37.52 ± 1.96^{bc}

CS-MPE2	26.87 ± 1.12^{c}	33.18 ± 1.74^{ab}
CS-MPE3	24.13 ± 0.97^{b}	28.74 ± 1.83^{a}

Different lowercase superscript letters indicate significant differences within a column ($p < 0.05$).

Application of Chitosan–MPE Coatings to Fresh Chicken Meat

pH

The changes in the pH of chicken meat during refrigerated storage are shown in Table 8. Two-way ANOVA showed significant effects of coating treatment ($F_{3,40} = 87.43$, $p < 0.001$), storage time ($F_{4,40} = 312.67$, $p < 0.001$), and their interaction ($F_{12,40} = 14.82$, $p < 0.001$). Thus, comparisons of treatments were made within storage days due to interaction. There was no difference between treatments in initial pH on day 0. In all treatments, pH rose over time but this rise was less in coatings containing MPE. By day 12, pH reached 6.84 ± 0.07 in the water control, compared with 6.61 ± 0.05, 6.47 ± 0.06, and 6.34 ± 0.04 in CS, CS-MPE1, and CS-MPE2, respectively. The lower pH recorded for coatings containing MPE was in agreement with the antibacterial activity and lower TVC values. Similar results of chitosan-based coating with plant-based active ingredients on pH changes during the refrigerated storage of chicken have been reported in the literature. Some coatings made of chitosan can inhibit microbial growth and the associated biochemical modification during refrigerated storage, while the level of inhibition varies depending on the composition of the chitosan coating and the storage conditions (Elsabee and Abdou, 2013; Muñoz-Tebar et al., 2023).

Table 8. pH of coated chicken meat during storage at 4°C (n = 3 biological replicates per treatment × day).

Day	Water	CS	CS-MPE1	CS-MPE2
0	5.84 ± 0.04^{a,A}	5.82 ± 0.03^{a,A}	5.83 ± 0.05^{a,A}	5.81 ± 0.04^{a,A}
3	6.04 ± 0.05^{a,B}	5.97 ± 0.04^{ab,B}	5.92 ± 0.04^{b,AB}	5.88 ± 0.03^{b,A}
6	6.31 ± 0.06^{a,c}	6.18 ± 0.05^{b,c}	6.08 ± 0.04^{c,B}	5.98 ± 0.04^{d,AB}
9	6.58 ± 0.07^{a,D}	6.42 ± 0.06^{b,D}	6.24 ± 0.05^{c,c}	6.14 ± 0.05^{d,B}
12	6.84 ± 0.07^{a,E}	6.61 ± 0.05^{b,E}	6.47 ± 0.06^{c,D}	6.34 ± 0.04^{d,c}

Different lowercase superscript letters within a row indicate significant differences among treatments at the same storage day. Different uppercase superscript letters within a column indicate significant differences among storage days within the same treatment ($p < 0.05$).

Water Retention Capacity

Water retention decreased progressively during refrigerated storage in all treatments. However, the coated samples retained more water than the water control, with the difference becoming more pronounced as storage progressed. At day 12, water retention was 54.32% in the water control, compared with 61.28%, 68.74%, and 72.87% for CS, CS-MPE1, and CS-MPE2, respectively (Table 9). The results suggest that the coatings might have resulted in higher retention of sample mass in the centrifugation-based test. For the coated chicken meat, the preservation of physicochemical quality during refrigerated storage has been reported for a chitosan-based coating system.

Table 9. Water retention (%) of coated chicken meat during refrigerated storage at 4°C.

Day	Water	CS	CS-MPE1	CS-MPE2
0	$78.52 \pm 1.52^{a,D}$	$78.52 \pm 1.48^{a,D}$	$78.52 \pm 1.55^{a,D}$	$78.52 \pm 1.50^{a,D}$
3	$72.61 \pm 1.47^{a,c}$	$74.83 \pm 1.43^{a,c}$	$75.96 \pm 1.51^{a,c}$	$76.84 \pm 1.38^{a,c}$
6	$65.37 \pm 1.53^{a,B}$	$70.21 \pm 1.46^{b,B}$	$73.14 \pm 1.49^{bc,bc}$	$74.92 \pm 1.44^{c,c}$
9	$59.83 \pm 1.58^{a,A}$	$65.74 \pm 1.52^{b,A}$	$70.86 \pm 1.46^{c,B}$	$73.95 \pm 1.41^{d,Bc}$
12	$54.32 \pm 1.61^{a,A}$	$61.28 \pm 1.55^{b,A}$	$68.74 \pm 1.43^{c,A}$	$72.87 \pm 1.37^{d,B}$

Different lowercase superscript letters within a row indicate significant differences among treatments. Different uppercase superscript letters within a column indicate significant differences among storage days ($p < 0.05$).

TBARS

Table 10 shows the TBARS results. Significant effects of coating treatment ($F_{3,40} = 124.36$, $p < 0.001$), storage time ($F_{4,40} = 418.74$, $p < 0.001$), and treatment × storage-time interaction ($F_{12,40} = 21.53$, $p < 0.001$) were observed. There was a gradual rise in TBARS in all treatments, suggesting a progressive increase in lipid oxidation during refrigerated storage. The percent increase varied between treatments. At day 12, the water control showed the highest TBARS value (2.87 ± 0.12 mg MDA/kg), followed by CS (1.98 ± 0.09 mg MDA/kg), CS-MPE1 (1.57 ± 0.08 mg MDA/kg), and CS-MPE2 (1.24 ± 0.07 mg MDA/kg). At day 12, the TBARS value of the CS-MPE2 treatment was thus 56.8% lower compared to the water control. The antioxidant activity in the film assays was confirmed by the lower TBARS values achieved in the treatments containing MPE. The same decrease in lipid oxidation has been observed for chitosan coatings loaded with antioxidant plant extracts used to preserve chicken meat during refrigerated storage (Mahdavi et al., 2018; Mehdizadeh & Mojaddar Langroodi, 2019; Zhang et al., 2020). Chitosan-based active coatings, thus, could serve as a physical barrier and also as a carrier system for antioxidant compounds; nonetheless, a separation of the contribution of the individual components is not possible without additional mechanistic experiments (Elsabee and Abdou, 2013; Muñoz-Tebar et al., 2023). The current experiment does not directly prove that the reduction of lipid oxidation is due to a molecular mechanism.

Table 10. TBARS values (mg MDA/kg) of coated chicken meat during storage at 4°C.

Day	Water	CS	CS-MPE1	CS-MPE2
0	$0.38 \pm 0.03^{a,A}$	$0.37 \pm 0.03^{a,A}$	$0.36 \pm 0.02^{a,A}$	$0.35 \pm 0.03^{a,A}$
3	$0.82 \pm 0.05^{a,B}$	$0.64 \pm 0.04^{b,B}$	$0.51 \pm 0.04^{c,B}$	$0.46 \pm 0.03^{c,B}$
6	$1.34 \pm 0.08^{a,c}$	$1.03 \pm 0.07^{b,c}$	$0.78 \pm 0.06^{c,c}$	$0.67 \pm 0.05^{d,c}$
9	$2.13 \pm 0.10^{a,D}$	$1.52 \pm 0.08^{b,D}$	$1.08 \pm 0.07^{c,D}$	$0.93 \pm 0.06^{d,D}$
12	$2.87 \pm 0.12^{a,E}$	$1.98 \pm 0.09^{b,E}$	$1.57 \pm 0.08^{c,E}$	$1.24 \pm 0.07^{d,E}$

Different lowercase superscript letters within a row indicate significant differences among treatments. Different uppercase superscript letters within a column indicate significant differences among storage days ($p < 0.05$).

Total Viable Count

The values of TVC are displayed in Table 11. Significant effects were observed for coating treatment ($F_{3,40} = 98.54$, $p < 0.001$), storage time ($F_{4,40} = 524.38$, $p < 0.001$), and the treatment × storage-time interaction ($F_{12,40} = 18.27$, $p < 0.001$). There was no difference in the initial TVC (3.16 to 3.24 log CFU/g) between treatments at day 0. The increase in the microbial counts was gradual for all treatments, but at a lower rate in coated treatments with the lowest rate in the treatment containing MPE. At day 12, the water control reached 8.63 ± 0.21 log CFU/g, compared with 7.84 ± 0.17 log CFU/g for CS, 6.94 ± 0.15 log CFU/g for CS-MPE1, and 6.38 ± 0.13 log CFU/g for CS-MPE2. At day 12, CS-MPE2 decreased the observed TVC by ~2.25 log CFU/g compared to the water control. The smaller number of microbes in the coatings with MPE correlates with the antibacterial activity measured in the film assay. Previous studies have also revealed that plant extracts and/or essential oils

incorporated in chitosan-based coatings can inhibit microbial growth in refrigerated chicken meat (Afshar Mehrabi et al., 2021; Mehdizadeh & Mojaddar Langroodi, 2019; Pires et al., 2022; Yaghoubi et al., 2021). Artemisia fragrans essential oil and chitosan coatings decreased TVC during the refrigerated storage of chicken, and chitosan and Nepeta pogonosperma extract decreased the TVC and several microbial groups during the chilled storage of the chicken (Afshar Mehrabi et al., 2021; Yaghoubi et al., 2021; Kongboonkird et al., 2026). However, TVC is used as an indicator of total culturable aerobic microorganisms, and it does not differentiate among the microorganisms that cause spoilage or pathogens.

Table 11. Total viable count (log CFU/g) of coated chicken meat during storage at 4°C.

Day	Water	CS	CS-MPE1	CS-MPE2
0	$3.24 \pm 0.12^{a,A}$	$3.21 \pm 0.11^{a,A}$	$3.18 \pm 0.13^{a,A}$	$3.16 \pm 0.12^{a,A}$
3	$4.47 \pm 0.14^{a,B}$	$4.12 \pm 0.13^{ab,B}$	$3.84 \pm 0.12^{bc,B}$	$3.63 \pm 0.11^{c,B}$
6	$5.83 \pm 0.16^{a,c}$	$5.24 \pm 0.14^{b,c}$	$4.76 \pm 0.13^{c,c}$	$4.42 \pm 0.12^{d,c}$
9	$7.24 \pm 0.18^{a,D}$	$6.73 \pm 0.15^{b,D}$	$5.87 \pm 0.14^{c,D}$	$5.34 \pm 0.13^{d,D}$
12	$8.63 \pm 0.21^{a,E}$	$7.84 \pm 0.17^{b,E}$	$6.94 \pm 0.15^{c,E}$	$6.38 \pm 0.13^{d,E}$

Different lowercase superscript letters within a row indicate significant differences among treatments. Different uppercase superscript letters within a column indicate significant differences among storage days ($p < 0.05$).

CONCLUSION

The results of this study showed that the physicochemical properties and functional characteristics of chitosan films were significantly altered due to the incorporation of mango peel extract (MPE). As the concentration of MPE increased, its antioxidant and antibacterial properties, opacity, swelling and solubility improved, and its moisture content and water-vapor permeability decreased. The FTIR, XRD, SEM and TGA analyses also showed that the molecular environment, structural organization, surface morphology and thermal behaviour of the films also vary with concentration. The use of chitosan–MPE coatings in fresh chicken breast meat postponed the deterioration of the quality characteristics during refrigerated storage at 4 ± 1°C, determined by pH value, TBARS, water retention and total viable counts when compared to the water control. Among the formulations evaluated on chicken meat, CS-MPE2 showed the greatest overall preservation effect, with lower TBARS and total viable counts and higher water retention during refrigerated storage. MPE shows potential as a bioactive component of chitosan-based coatings for improving the refrigerated storage stability of fresh chicken meat.

Declarations

Author contributions: Sourav Kumar Biswas, Md. Maruf Shaikh, Rahul Nandi, Monyer Abdulameir Abd Alfatlawi, Muhammad Hamza Sardar, Sehrish Murtaza, Tareq Nayef AlRamadneh, Saira Rehman and Izhar Ullah Shah contributed equally to the conceptualization, methodology, investigation, data analysis, writing, review, and editing of the manuscript. All authors read and approved the final version of the manuscript.

Funding: The authors declare that no funds, grants, or other support were received during the preparation of this manuscript.

Data availability: Adequate data have been provided in the form of tables and figures.

Conflict of interest: No conflict of interest

Acknowledgment: No Acknowledgment

REFERENCES

[1] Adilah, A.N., Jamilah, B., Mohd Adzahan, N., Zainal Abedin, N.H., 2018. Utilization of mango peel extracts on the biodegradable films for active packaging. *Food Packaging and Shelf Life* 16, 1–7. https://doi.org/10.1016/j.fpsl.2018.01.006

[2] Afshar Mehrabi, F., Sharifi, A., Ahvazi, M., 2021. Effect of chitosan coating containing *Nepeta pogonosperma* extract on shelf life of chicken fillets during chilled storage. *Food Science & Nutrition* 9, 4517–4528. https://doi.org/10.1002/fsn3.2429

[3] Aider, M., 2010. Chitosan application for active bio-based films production and potential in the food industry: Review. *LWT–Food Science and Technology* 43, 837–842. https://doi.org/10.1016/j.lwt.2010.01.021

[4] Ajila, C.M., Bhat, S.G., Prasada Rao, U.J.S., 2007. Valuable components of raw and ripe peels from two Indian mango varieties. *Food Chemistry* 102, 1006–1011. https://doi.org/10.1016/j.foodchem.2006.06.036

[5] Bi, F., Zhang, X., Bai, R., Liu, Y., Liu, J., Liu, J., 2019. Preparation and characterization of antioxidant and antimicrobial packaging films based on chitosan and proanthocyanidins. *International Journal of Biological Macromolecules* 134, 11–19. https://doi.org/10.1016/j.ijbiomac.2019.05.042

[6] Cazón, P., Vázquez, M., 2019. Mechanical and barrier properties of chitosan combined with other components as food packaging film. *Environmental Chemistry Letters* 18, 257–267. https://doi.org/10.1007/s10311-019-00936-3

[7] Cheng, J., Lin, X., Wu, X., Liu, Q., Wan, S., Zhang, Y., 2021. Preparation of a multifunctional silver nanoparticles polylactic acid food packaging film using mango peel extract. *International Journal of Biological Macromolecules* 188, 678–688. https://doi.org/10.1016/j.ijbiomac.2021.07.161

[8] El-Sayed, S.M., Abd-Elhalim, B.T., El-Dougdoug, K.A., Gamal, R.F., El-Bana, G.G., Mohamed, N.N.I., 2025. In vitro investigation of *Mangifera indica* L. peel extracts: Antibacterial, antioxidant, and docking studies. *AMB Express* 15, 73. https://doi.org/10.1186/s13568-025-01882-w

[9] Elsabee, M.Z., Abdou, E.S., 2013. Chitosan based edible films and coatings: A review. *Materials Science and Engineering: C* 33, 1819–1841. https://doi.org/10.1016/j.msec.2013.01.010

[10] Hamed, I., Özogul, F., Regenstein, J.M., 2016. Industrial applications of crustacean by-products (chitin, chitosan, and chitooligosaccharides): A review. *Trends in Food Science & Technology* 48, 40–50. https://doi.org/10.1016/j.tifs.2015.11.007

[11] Jahurul, M.H.A., Zaidul, I.S.M., Ghafoor, K., Al-Juhaimi, F.Y., Nyam, K.L., Norulaini, N.A.N., Sahena, F., Mohd Omar, A.K., 2015. Mango (*Mangifera indica* L.) by-products and their valuable components: A review. *Food Chemistry* 183, 173–180. https://doi.org/10.1016/j.foodchem.2015.03.046

[12] Kanatt, S.R., Chawla, S.P., 2018. Shelf life extension of chicken packed in active film developed with mango peel extract. *Journal of Food Safety* 38, e12385. https://doi.org/10.1111/jfs.12385

[13] Kerch, G., 2015. Chitosan films and coatings prevent losses of fresh fruit nutritional quality: A review. *Trends in Food Science & Technology* 46, 159–166. https://doi.org/10.1016/j.tifs.2015.10.010

[14] Khan, A.A., Arshad, M., Mujahid, T., Yaqoob, R., Asghar, S., Ahmed, H.A., Tahir, Z., Qamar, W., Tahir, I., 2026a. Autophagy and apoptosis in the survival of cancer cells. In: Altaf, S., Jahan, N., Kabeer, R. (Eds.), *Cancer biology and precision oncology: Innovations in diagnosis, drug discovery and therapy*. Unique Scientific Publishers, pp. 277–283. https://doi.org/10.47278/book.TL/2026.461

[15] Khan, A.A., Fatima, H., Alkhasaky, A., Bobokulov, N., Riaz, N., Sadikan, M.Z., Abdullah, A., 2026b. In silico design and evaluation of CRISPR-Cas9 guide RNAs targeting the HTT gene for Huntington's disease therapy. *International Journal of Drug Delivery Technology* 16, 23–31. https://doi.org/10.25258/ijddt.16.25s.4

[16] Khan, A.A., Waheed, M., Bangash, S.A., Gupta, A., o'g'li, I.D.A., 2026c. Targeted drug delivery systems using nanoparticles. *International Journal of Drug Delivery Technology* 16, 510–518. https://doi.org/10.25258/ijddt.16.36s.59

[17] Khan, A.A., Arooj, S., Shabbir, S., Errum, A., Virk, R., Rahmat, S.A., 2026d. The role of gut microbiota in kidney health and disease. *International Journal of Drug Delivery Technology* 16, 62–73. https://doi.org/10.25258/ijddt.16.21s.7

[18] Kongboonkird, M., Chatraphorn, S., Lee, Y.S., Iwamoto, S., Siripatrawan, U., 2026. Sustainable active packaging from cold plasma-treated chitosan film loaded with cinnamon oil nanoemulsion for preserving fresh chicken meat quality. *International Journal of Biological Macromolecules* 368, 152561. https://doi.org/10.1016/j.ijbiomac.2026.152561

[19] Mahdavi, V., Hosseini, S.E., Sharifan, A., 2018. Effect of edible chitosan film enriched with anise (*Pimpinella anisum* L.) essential oil on shelf life and quality of the chicken burger. *Food Science & Nutrition* 6, 269–279. https://doi.org/10.1002/fsn3.544

[20] Marçal, S., Pintado, M., 2021. Mango peels as food ingredient/additive: Nutritional value, processing, safety and applications. *Trends in Food Science & Technology* 114, 472–489. https://doi.org/10.1016/j.tifs.2021.06.012

[21] Mehdizadeh, T., Mojaddar Langroodi, A., 2019. Chitosan coatings incorporated with propolis extract and *Zataria multiflora* Boiss oil for active packaging of chicken breast meat. *International Journal of Biological Macromolecules* 141, 401–409. https://doi.org/10.1016/j.ijbiomac.2019.08.267

[22] Moalla, S., Ammar, I., Fauconnier, M.-L., Danthine, S., Blecker, C., Besbes, S., Attia, H., 2021. Development and characterization of chitosan films carrying *Artemisia campestris* antioxidants for potential use as active food packaging materials. *International Journal of Biological Macromolecules* 183, 254–266. https://doi.org/10.1016/j.ijbiomac.2021.04.113

[23] Mujtaba, M., Morsi, R.E., Kerch, G., Elsabee, M.Z., Kaya, M., Labidi, J., Khawar, K.M., 2019. Current advancements in chitosan-based film production for food technology: A review. *International Journal of Biological Macromolecules* 121, 889–904. https://doi.org/10.1016/j.ijbiomac.2018.10.109

[24] Muñoz-Tebar, N., Pérez-Álvarez, J.A., Fernández-López, J., Viuda-Martos, M., 2023. Chitosan edible films and coatings with added bioactive compounds: Antibacterial and antioxidant properties and their application to food products: A review. *Polymers* 15, 396. https://doi.org/10.3390/polym15020396

[25] Pires, J.R.A., Almeida, K.M., Augusto, A.S., Vieira, É.T., Fernando, A.L., Souza, V.G.L., 2022. Application of biocomposite films of chitosan/natural active compounds for shelf life extension of fresh poultry meat. *Journal of Composites Science* 6, 342. https://doi.org/10.3390/jcs6110342

[26] Ponnusamy, A., Khan, A., Prodpran, T., Kim, J.T., Benjakul, S., Rhim, J.-W., 2025. Active packaging film based on chitosan/gelatin blend incorporated with mango peel carbon dots: Properties and shelf life extension of minced pork. *International Journal of Biological Macromolecules* 288, 138692. https://doi.org/10.1016/j.ijbiomac.2024.138692

[27] Priyadarshi, R., Sauraj, Kumar, B., Negi, Y.S., 2018. Chitosan film incorporated with citric acid and glycerol as an active packaging material for extension of green chilli shelf life. *Carbohydrate Polymers* 195, 329–338. https://doi.org/10.1016/j.carbpol.2018.04.089

[28] Quintana, S.E., Salas, S., García-Zapateiro, L.A., 2021. Bioactive compounds of mango (*Mangifera indica*): A review of extraction technologies and chemical constituents. *Journal of the Science of Food and Agriculture* 101, 6186–6192. https://doi.org/10.1002/jsfa.11455

[29] Rambabu, K., Bharath, G., Banat, F., Show, P.L., Hernández Cocoletzi, H., 2019. Mango leaf extract incorporated chitosan antioxidant film for active food packaging. *International Journal of Biological Macromolecules* 126, 1234–1243. https://doi.org/10.1016/j.ijbiomac.2018.12.196

[30] Ribeiro, A.C.B., Cunha, A.P., Ribeiro da Silva, L.M., Mattos, A.L.A., de Brito, E.S., de Souza Filho, M.S.M., Azeredo, H.M.C., Ricardo, N.M.P.S., 2021. From mango by-product to food packaging: Pectin-phenolic antioxidant films from mango peels. *International Journal of Biological Macromolecules* 193, 1138–1150. https://doi.org/10.1016/j.ijbiomac.2021.10.131

[31] Salgado, P.R., Ortiz, C.M., Musso, Y.S., Di Giorgio, L., Mauri, A.N., 2015. Edible films and coatings containing bioactives. *Current Opinion in Food Science* 5, 86–92. https://doi.org/10.1016/j.cofs.2015.09.004

[32] Sarfraz, M.H., Hayat, S., Siddique, M.H., Aslam, B., Ashraf, A., Saqalein, M., Khurshid, M., Sarfraz, M.F., Afzal, M., Muzammil, S., 2024. Chitosan based coatings and films: A perspective on antimicrobial, antioxidant, and intelligent food packaging. *Progress in Organic Coatings* 188, 108235. https://doi.org/10.1016/j.porgcoat.2024.108235

[33] Shin, D.-M., Kim, Y.-J., Yune, J.-H., Kim, D.-H., Kwon, H.-C., Sohn, H., Han, S.-G., Han, J.-H., Lim, S.-J., Han, S.-G., 2022. Effects of chitosan and duck fat-based emulsion coatings on the quality characteristics of chicken meat during storage. *Foods* 11, 245. https://doi.org/10.3390/foods11020245

[34] Sikapuria, Z.K., Khan, A.A., Abdullah, A., Batumi, A.A.A., Sadika, M.Z., Rasheed, M.M., 2026. A research study of determining adaptability of medication its factors among patients with chronic kidney disease, a prospective analysis how gut microbiome affect treatment cycle and quality of life of patients. *Genetics and Molecular Research*.

[35] Umamahesh, K., Gandhi, A.D., Reddy, O.V.S., 2020. Ethnopharmacological applications of mango (*Mangifera indica* L.) peel: A review. *Current Bioactive Compounds* 16, 1298–1303. https://doi.org/10.2174/1389201021666200420075759

[36] Wang, L., Guo, H., Wang, J., Jiang, G., Du, F., Liu, X., 2019. Effects of *Herba Lophatheri* extract on the physicochemical properties and biological activities of the chitosan film. *International Journal of Biological Macromolecules* 133, 51–57. https://doi.org/10.1016/j.ijbiomac.2019.04.067

[37] Yaghoubi, M., Ayaseh, A., Alirezalu, K., Nemati, Z., Pateiro, M., Lorenzo, J.M., 2021. Effect of chitosan coating incorporated with *Artemisia fragrans* essential oil on fresh chicken meat during refrigerated storage. *Polymers* 13, 716. https://doi.org/10.3390/polym13050716

[38] Yildirim, S., Röcker, B., Pettersen, M.K., Nilsen-Nygaard, J., Ayhan, Z., Rutkaite, R., Radusin, T., Suminska, P., Marcos, B., Coma, V., 2018. Active packaging applications for food. *Comprehensive Reviews in Food Science and Food Safety* 17, 165–199. https://doi.org/10.1111/1541-4337.12322

[39] Yuan, G., Chen, X., Li, D., 2016. Chitosan films and coatings containing essential oils: The antioxidant and antimicrobial activity, and application in food systems. *Food Research International* 89, 117–128. https://doi.org/10.1016/j.foodres.2016.10.004

[40] Zhang, H., Liang, Y., Li, X., Kang, H., 2020. Effect of chitosan-gelatin coating containing nano-encapsulated tarragon essential oil on the preservation of pork slices. *Meat Science* 166, 108137. https://doi.org/10.1016/j.meatsci.2020.108137

[41] Zhong, Y., Dong, L., Long, Y., He, Z., Xiao, H., 2026. Recent advances in chitosan-based packaging materials for active and intelligent food preservation. *Food Chemistry* 516, 149280. https://doi.org/10.1016/j.foodchem.2026.149280

[42] Roy, D., Nazeer, N., Khudoykulova, Z., et al., 2026. Chemical reduction–derived nickel nanoparticles as multifunctional antimicrobial and wound healing agents: Mechanistic, biocompatibility, and computational insights. *Biological Trace Element Research*. https://doi.org/10.1007/s12011-026-05152-z